Ultrahigh-Intensity Optical Slow-Wave Structure

B. D. Layer,[1,3] A. York,[1,3] T. M. Antonsen,[2,3] S. Varma,[1,2] Y.-H. Chen,[1,2] Y. Leng,[2] and H. M. Milchberg[1,2,3]

[1]*Institute for Physical Science and Technology, University of Maryland, College Park, Maryland 20742, USA*
[2]*Department of Electrical and Computer Engineering, University of Maryland, College Park, Maryland 20742, USA*
[3]*Department of Physics, University of Maryland, College Park, Maryland 20742, USA*

(Received 9 February 2007; published 19 July 2007)

We report the development of corrugated "slow-wave" plasma guiding structures with application to quasiphase-matched direct laser acceleration of charged particles and generation of a wide spectrum of electromagnetic radiation. These structures support guided propagation at intensities up to 2×10^{17} W/cm^2, limited by our current laser energy and side leakage. Hydrogen and argon plasma waveguides up to 1.5 cm in length with corrugation period as short as 35 μm are generated in a cryogenic cluster jet. Experimental data are consistent with simulations showing periodic modulations of the laser pulse intensity.

DOI: 10.1103/PhysRevLett.99.035001 PACS numbers: 52.38.Hb, 36.40.Gk, 36.40.Vz, 52.50.Jm

In the rapidly developing field of ultraintense laser-plasma interactions, applications including electron acceleration by laser-driven wakefields [1], x-ray lasers, and coherent electromagnetic wave generation [2] must rely for their fullest realization on the extended diffraction-suppressed propagation of extreme intensity laser pulses in plasma optical guiding structures. Plasma waveguides for intense optical pulses were first generated through the radial hydrodynamic shock expansion of picosecond laser-heated gas plasma [3]. Later, waveguides were demonstrated in electrical discharge capillaries [4], in variations of the hydrodynamic shock technique [5], and, most recently using laser-driven hydrodynamic shocks in cluster jet targets, both end pumped [6] and side pumped [7]. The optical mode structure and dispersion properties of plasma waveguides have been discussed in detail [8].

Waveguide control of beams can be augmented by additional "branches" to the ω versus k dispersion diagram, where $k = k(\omega)$ is the axial wave number of the guide and ω is the angular frequency. Adding an axial (z) modulation of period d gives rise to a wider class of solutions $u(\mathbf{r}_\perp, z, \omega)\exp(ikz)$ where $u(\mathbf{r}_\perp, z + d, \omega) = u(\mathbf{r}_\perp, z, \omega)$ and $k = k_c(\omega) + 2\pi m/d$ (from the Floquet-Bloch theorem), where u is an electromagnetic field component, $\mathbf{r}_\perp$ is transverse position, m is an integer, and k_c is the fundamental axial wave number [9].

For low intensity radiation beams, modulated guiding structures find wide application in both microwave sources and radio frequency (rf) accelerators [9,10]. In these "slow wave" structures fields have effective k values, as discussed above, that give phase velocities $v_p = \omega/k < c$, allowing particle and wave speeds to be matched. In contrast, in unmodulated, metal waveguides the phase velocity is superluminal, precluding strong interaction with the subluminal particle beams. Another view of this matched interaction—called *quasiphase matching*—is that the wave speeds up and slows down in successive half-periods of the modulation in such a way that the partial acceleration in the first half is not completely cancelled by deceleration in the second half. We note that for a number of applications, quasiphase matching is enabled not only by the modulations in linear dispersion, but also by the accompanying laser intensity modulations. In low-intensity guided wave optics, periodic modulation in the material's optical nonlinearity or refractive index makes possible the quasiphase matched generation of low-order harmonics of the fundamental pump wave [11]. At higher intensity ($\sim 10^{14}$–10^{15} W/cm^2), modulated, gas-filled hollow core fibers have been used for the generation of extreme ultraviolet high harmonics [12]. Recent work [13] has shown that the propagation of an intense pulse over several plasma segments with total extent <1 mm could assist the phase matching of third-order harmonic generation. However, quasiphase matching becomes important only after diffraction is removed as a limiting factor. Without the direct measurement of plasma density profiles, energy throughputs, guided laser spot sizes, or guiding itself, it is unclear if that experiment [13] effectively extended the nonlinear interaction beyond a Rayleigh length.

In this Letter, we demonstrate for the first time high intensity optical guiding in an extended corrugated plasma slow-wave structure. Such plasma structures, which can be used for direct laser acceleration of charged particles or quasiphase matched coherent electromagnetic wave generation, were first discussed in Ref. [14]. Spontaneous, but uncontrolled, modulated channels were reported in Ref. [15]. Here we have produced exceptionally stable plasma waveguides with adjustable axial modulation periods as short as 35 μm, where the period can be significantly smaller than the waveguide diameter. We have measured guided propagation at intensities up to 2×10^{17} W/cm^2, limited only by our current laser energy and waveguide leakage.

Figure 1 shows the experimental setup. Initially, unmodulated waveguides were generated in cluster jets [7] using lowest-order (J_0) Bessel beam pulses produced by an axicon-focused beam from a 10 Hz, 1064 nm, 100 ps Nd:YAG laser with pulse energy of 200–500 mJ.

The cluster source in these experiments was a cryogenically cooled supersonic gas jet with a 1.5 cm long by 1 mm wide nozzle exit orifice. Clusters form when a highly pressurized gas expands through the nozzle into vacuum, with the atoms or molecules attracted to one another by van der Waals forces. Aggregates form at solid density with diameter 1–50 nm ($\sim 10^2$–10^7 atoms), depending on nozzle geometry, gas species, and jet backing temperature and pressure, which were controlled in the range 115–295 K and 100–1000 psi. The 25 mm line-focus length of the Bessel beam overlapped the 1.5 cm length of the cluster jet, resulting in 1.5 cm long plasma channels. Waveguides were injected at $f/10$ through a hole in the axicon [Fig. 1(a)] with a 70 mJ, 70 fs, 800 nm Ti:sapphire laser pulse synchronized [16] and delayed with respect to the channel-generating Nd:YAG pulse. A small portion of this pulse ($\sim$1 mJ) was split off into a delay line, directed transversely through the waveguide, and then imaged through a femtosecond folded wave front Michelson interferometer onto a CCD camera. Electron density profile images of the evolving corrugated waveguide were obtained by phase extraction of the time-resolved interferograms, followed by Abel inversion.

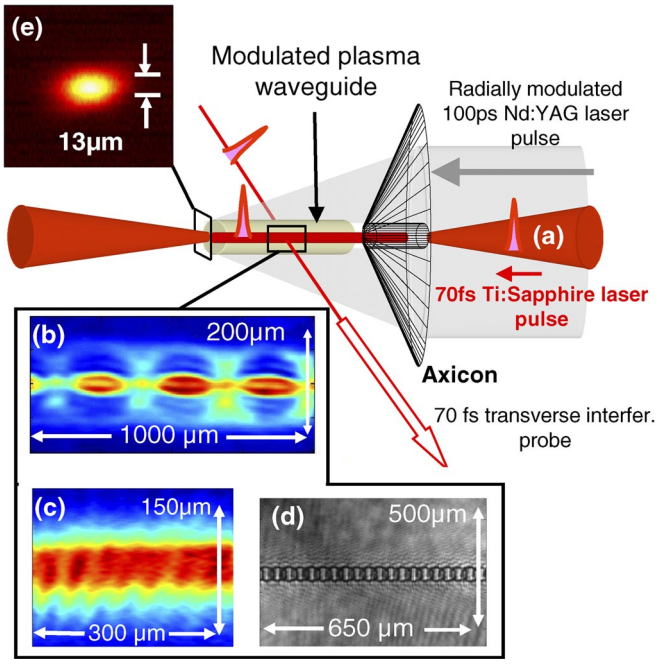

FIG. 1 (color online). Experimental geometry: radially modulated Nd:YAG laser pulse (200–500 mJ, 100 ps, 1064 nm) from ring grating imaging system (not shown) focused by an axicon onto a liquid nitrogen-cooled elongated cluster jet target, generating a 1.5 cm long corrugated plasma channel. (a) Ti:sapphire laser pulse guided down the channel at an adjustable delay with respect to the Nd:YAG pulse. A 1 mJ portion of the 70 fs, 800 nm pulse was directed transversely through the corrugated guide and into a folded wave front Michelson interferometer for time-resolved interferrometric/shadowgraphic images. Phase images of channels with (b) 300 μm and (c) 35 μm modulation periods in argon cluster targets and (d) a 35 μm period in air. (e) Lowest-order exit mode from the guide of Fig. 3(b), panel (1ii), with $w_{\mathrm{HWHM}} = 13$ μm.

We have shown previously [7] that the use of clusters can increase the 100 ps Bessel beam absorption efficiency by an order of magnitude compared to unclustered gas targets of the same volume average density. This high absorption efficiency occurs in spite of the fact that typical clusters in this experiment (size $\sim$5–30 nm) explosively disassemble and expand below the plasma critical density on a subpicosecond time scale [17]. With cluster targets the far leading edge of the 100 ps pulse prepares a highly ionized, locally uniform, and cool plasma from the expanded and merged individual cluster plasmas, which the remainder of the pulse can heat efficiently [7].

To impose axial modulations upon the plasma channel, a transmissive ''ring grating'' (RG) and associated imaging optics were centered in the path of the Nd:YAG laser pulse. The RG used in these experiments was a 1 in. diameter, lithographically etched fused silica disk with variable groove period, groove structure, and duty cycle. The axicon projects the diffraction pattern produced by the RG onto the optical axis, leading to axial intensity modulations of the Bessel beam. The dominant axial modulation of the central spot intensity imposes axial modulations in the heating and plasma generation in the cluster jet.

The 100 ps heater pulse is essentially an impulse on the hydrodynamic time scale ($\sim$0.1–0.5 ns) of the heated bulk plasma (formed from merged cluster explosions) that remains after the pulse [7]. This plasma then undergoes axially periodic radial hydrodynamic shock expansion, producing a corrugated plasma waveguide. Examples of two phase images of the magnified central waveguide region are shown in Figs. 1(b) and 1(c), with modulation periods of 300 and 35 μm, using two different RGs and an argon cluster jet. Corrugated guides can also be generated in backfill gases: Fig. 1(d) shows a shadowgram of a modulated channel produced in air with a period of 35 μm. A typical guided exit mode from a modulated cluster plasma channel (half width at half maximum mean radius 13 μm) is shown in Fig. 1(e). Note that the cluster-generated channels are highly stable and reproducible: all density profiles shown in this Letter are extracted from the average phase of 200 consecutive interferograms. The shot-to-shot extracted density variation is less than 5%.

Figure 2 shows results for a corrugated hydrogen plasma waveguide. Hydrogen plasma waveguides are attractive for laser-plasma acceleration [1] because they are easily fully ionized during their formation, making impossible further ionization by guided intense pulses, which can lead to distortion and ionization-induced refractive defocusing. The modulation period $d \sim 300$ μm was chosen to ensure clearly observable periodic oscillations in laser intensity. Figure 2(a) shows the electron density $N_e(r, z)$ of a 3 mm section near the entrance of a 1.5 cm hydrogen waveguide, 1 ns after generation. The density profiles are very similar in the injected and uninjected waveguides, showing that little change to the guide was produced by the guided

pulse. With modulated hydrogen guides, energy throughput is ~10%, yielding output intensity of 10^{17} W/cm^2. The low throughput is due to leakage and side scattering out of the guide due to the modulations. This leakage is directly seen in argon results and simulations presented later in the Letter. Figure 2(b) shows higher magnification profiles of two modulation periods as a function of interferometer probe pulse delay (0.5, 1, and 2 ns), for channel creation pulse energies of (i) 200 mJ and (ii) 300 mJ. It is seen that lower pulse energy [(i)] can produce periodic "beads" of plasma, separated by zones of neutral clusters/atoms, while higher energy [(ii)] results in a more continuous channel. The beads act as plasma lenslets, collecting the light emerging from a neutral gap and focusing the beam into the next gap.

Channels with higher ionization Z were generated in argon cluster jets. Figure 3(a) shows an extended region of channel at 1.5 ns delay with and without guided pulse injection (bottom and top panels, respectively) for a probe delay ~10 ps after guided pulse passage. It is seen that the channel itself is little affected by the guided pulse, but in contrast to the hydrogen results, there is a significant electron density "halo" located at a radial distance ~100 μm from the channel. Short interval sequences of probe images show that the halo propagates right to left at the speed of light with the guided pulse. The halo radial position remains constant over the full 1.5 cm length of the corrugated channel but decays in density, suggesting that it originates from additional cluster ionization from channel side leakage [8] rather than from uncoupled entrance light skimming the outside of the channel. The leakage light moves radially across a zone of low density plasma and neutrals until it reaches the layer of argon clusters that was unperturbed during channel formation. With hydrogen, the clusters are smaller and more fragile, so it is unlikely they survive so close to the channel after its formation, and hence there is no observed halo in Fig. 2.

Higher resolution images of 3 periods of modulation near the argon channel center are shown in Fig. 3(b), for cases of beaded (300 mJ pump, left column) and continuous (500 mJ pump, right column) modulations, without guided pulse injection [panels (1)] and with injection [panels (2) and (3)]. In the case of the beaded guide, Fig. 3(b) [panel (2i)] shows strong additional ionization by the guided pulse in the neutral gaps as the beam is focused by each plasma lenslet and collected by the next. Remarkably, in this case, the overall channel coupled energy throughput is still 10%, showing that there is significant injection/capture of light by successive lenslets over the full 1.5 cm length of the channel. Throughput for the continuous modulation case is 20%, yielding 2×10^{17} W/cm^2 peak intensity at a beam waist, using the fact that the beam exits the channel at a guide bulge. By comparison, throughput for this injection delay in unmodulated waveguides is 60%. Panels (2) both show in more detail the ionization halo induced by side leakage of the guided pulse. Side-imaged Thomson-Rayleigh scattering of guided 800 nm light shows scattering strongly localized

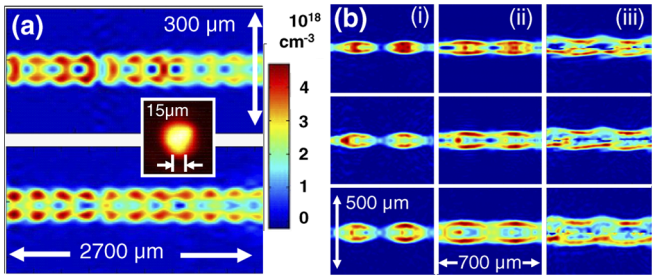

FIG. 2 (color online). Corrugated channels produced in a hydrogen cluster jet at 800 psi and −145 °C backing pressure and temperature. (a) ~3 mm section of channel without (top panel) and with (bottom panel) injection at 1 ns delay of a 70 mJ, 70 fs, 800 nm laser pulse, viewed 100 ps after pulse passage. The channel exit mode of $w_{\mathrm{HWHM}} = 15$ μm is shown in the inset. (b) Higher magnification Abel-inverted electron density profiles of 2 corrugation periods for channel creation pulse energies of (i) 200 mJ, (ii) 300 mJ, and (iii) 500 mJ (with intentional RG/axicon misalignment) at interferometer probe delays of, top to bottom, 0.5, 1, and 2 ns.

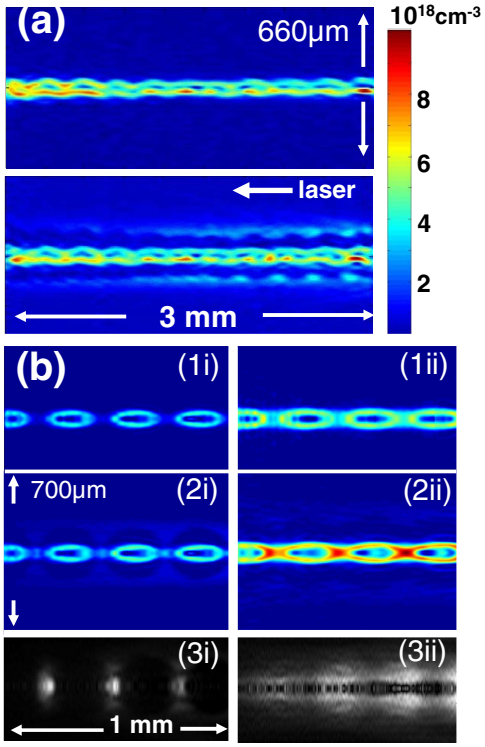

FIG. 3 (color online). Corrugated channels in an argon cluster jet at 800 psi backing pressure and room temperature. Laser 70 mJ, 70 fs, 800 nm. (a) 3 mm section of channel without (top panel) and with (bottom panel) injection at 1.5 ns delay. (b) Magnified images at 2 ns delay of beaded (300 mJ pump, left column) and more continuous (500 mJ pump, right column) channel modulations. Left and right columns: (1) density profile of uninjected guide, (2) density profile of injected guide, (3) Abel-inverted scattering image at 800 nm corresponding to (2).

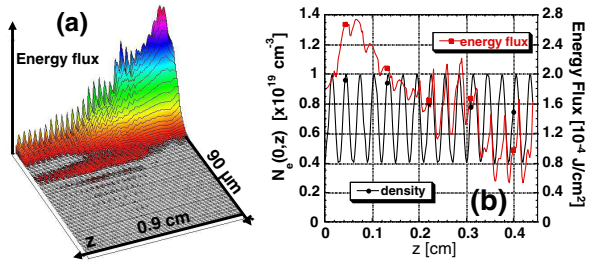

FIG. 4 (color online). Simulation using the code WAKE [18]. (a) Surface plot of the radial and axial dependence of the energy flux (J/cm^2). The vertical scale is given in (b). (b) Plot of the on axis ($r = 0$) energy flux and electron density plotted versus axial distance.

from cluster ionization at the neutral gaps in the beaded guide [Fig. 3(b), panel (3i)], and more smoothly modulated from leakage at the beam waists in the more continuous guide [Fig. 3(b), panel (3ii)]. These images make clear that the dominant scatterers are likely clusters, either those surviving in the gaps between beads or those external to the continuously modulated guide.

To better understand the propagation dynamics, we performed simulations using our intense laser pulse propagation code WAKE [18]. Propagation of an injected 60 mJ, 70 fs pulse over a distance of 0.9 cm, corresponding to 30 periods of the structure, was simulated using $N_e(r, z)$ for the case of the argon channel shown in Fig. 3(b), panel (2ii). Channel leakage is shown in Fig. 4(a), a surface plot of the energy flux $S(r, z) \propto \int_{-\infty}^{\infty} I(r, z)dt$, where I is the laser intensity. The simulated guide throughput of 27% is due to leakage from the channel and simulation volume, corresponding to an exponential leakage coefficient of $\gamma = 1.4\ \mathrm{cm}^{-1}$. This is in good agreement with the experimental result corresponding to Fig. 3(b), panel (2ii), for which $\gamma = 1.4\ \mathrm{cm}^{-1}$ after the 60% input coupling efficiency is accounted for. The channel causes modulations in the energy flux that are also seen in the experiment, Fig. 3(b), panel (3ii). These modulations are plotted for a smaller range of axial distance in Fig. 4(b) and are seen to be correlated with the variations in the on axis electron density, demonstrating the focusing-defocusing properties of the channel.

The large oscillations of intensity and phase due to the axially modulating guide parameters give rise to slow-wave components of the laser field with phase velocity $v_p/c = 1 - m\lambda/d + \bar{N}_e/(2N_{\mathrm{cr}}) + 2\lambda^2/(2\pi w)^2$, where w is the $1/e$ field radius of the guided mode, $\bar{N}_e$ is the average electron density on axis, $\lambda = 2\pi/k_0$ is the laser vacuum wavelength, and N_{cr} is the critical density [19]. For the measured parameters ($w = 15\ \mu$m, $\bar{N}_e/N_{\mathrm{cr}} = 4 \times 10^{-3}$, $l/d = 2.7 \times 10^{-3}$), $m \geq 1$ is required for a subluminal phase velocity. If the dominant contribution to the generation of slow spatial harmonics comes from the variation of the wave phase ϕ from sinusoidal density modulations of relative amplitude δ, then $d\phi/dz = -k_0\alpha\cos(2\pi z/d)$, where $\alpha = \delta\bar{N}_e/(2N_{\mathrm{cr}})$ and the ratio of the amplitude of the mth spatial harmonic to the local field amplitude is $E_m/|E| = J_m(\alpha d/\lambda)$, where J_m is the ordinary Bessel function. The magnitude of a given spatial harmonic can thus be maximized by the appropriate choice of the density modulations and their period. In the case of Fig. 3(b), panel (2ii), $\delta = 0.43$ gives $\alpha d/\lambda = 0.32$. Thus, the relative amplitude of the first slow-wave harmonic is $J_1(0.32) \sim 0.16$, for which $(1 - v_p/c) = 5.2 \times 10^{-4}$ and relativistic $\gamma \sim 30$.

In conclusion, we have demonstrated guiding and dispersive control of intense laser pulses in miniature plasma slow-wave guiding structures, making possible both particle and photon applications based on quasiphase matching. Our corrugated channel generation scheme, which exploits the unique properties of clusters and cluster plasmas, makes possible control of the dominant axial spatial harmonics of the driving or pump waves.

This work was supported by the U.S. Department of Energy and the National Science Foundation. The authors thank C. Pesto for technical assistance.

[1] T. Tajima and J. M. Dawson, Phys. Rev. Lett. **43** 267 (1979); E. Esarey *et al.*, IEEE Trans. Plasma Sci. **24**, 252 (1996).
[2] A. Butler *et al.*, Phys. Rev. Lett. **91**, 205001 (2003); D. V. Korobkin *et al.*, *ibid.* **77**, 5206 (1996); H. M. Milchberg *et al.*, J. Opt. Soc. Am. B **12**, 731 (1995); H. M. Milchberg *et al.*, Phys. Rev. Lett. **75**, 2494 (1995).
[3] C. G. Durfee, J. Lynch, and H. M. Milchberg, Phys. Rev. E **51**, 2368 (1995).
[4] Y. Ehrlich *et al.*, Phys. Rev. Lett. **77** 4186 (1996); A. Butler *et al.*, Phys. Rev. Lett. **89**, 185003 (2002).
[5] P. Volfbeyn *et al.*, Phys. Plasmas **6** 2269 (1999); E. W. Gaul *et al.*, Appl. Phys. Lett. **77**, 4112 (2000).
[6] V. Kumarappan, K. Y. Kim, and H. M. Milchberg, Phys. Rev. Lett. **94**, 205004 (2005).
[7] H. Sheng *et al.*, Phys. Rev. E **72**, 036411 (2005).
[8] T. R. Clark and H. M. Milchberg, Phys. Rev. E **61**, 1954 (2000).
[9] L. Schachter, *Beam-Wave Interaction in Periodic and Quasi-Periodic Structures* (Springer, Berlin, 1997).
[10] http://www2.slac.stanford.edu/vvc/accelerators/structure.html.
[11] R. H. Stolen and H. W. K. Tom, Opt. Lett. **12**, 585 (1987); R. Kashyap, J. Opt. Soc. Am. B **6**, 313 (1989); M. Fejer *et al.*, IEEE J. Quantum Electron. **28**, 2631 (1992); S. Chao *et al.*, Opt. Express **13**, 7091 (2005).
[12] A. Paul *et al.*, Nature (London) **421**, 51 (2003).
[13] C.-C. Kuo *et al.*, Phys. Rev. Lett. **98**, 033901 (2007).
[14] H. M. Milchberg *et al.*, Phys. Plasmas **3**, 2149 (1996).
[15] J. Cooley *et al.*, Bull. Am. Phys. Soc. **45**, 237 (2000); J. Cooley *et al.*, Phys. Rev. E **73**, 036404 (2006).
[16] S. Nikitin *et al.*, Phys. Rev. E **59**, R3839 (1999).
[17] K. Y. Kim *et al.*, Phys. Rev. Lett. **90**, 023401 (2003).
[18] P. Mora and T. M. Antonsen, Jr., Phys. Plasmas **4**, 217 (1997).
[19] A. York, B. D. Layer, and H. M. Milchberg, AIP Conf. Proc. **877**, 807 (2006).